

Batch and Continuous Flow Treatment Studies of Trichloroethylene Contaminated in Water by Silver and Cerium Doped Zinc Oxide Adsorption and Photocatalysis (Kajian Rawatan Kumpulan dan Aliran Berterusan Trikloroetilena Tercemar dalam Air oleh Perak dan Cerium Terdop Zink Oksida Penjerapan dan Fotopemangkinan)

SARTTRAWUT TULAPHOL^{1,5}, NURAK GRIDANURAK^{2,3}, FRANKLIN ANARIBA⁴, CHANTRA TONGCUMPOU⁵ & PUMMARIN KHAMDAHSAG^{5,*}

¹*Sustainable Polymer & Innovative Composite Materials Research Group, Department of Chemistry, Faculty of Science, King Mongkut's University of Technology Thonburi, Bangkok 10140, Thailand*

²*Department of Chemical Engineering, Faculty of Engineering, Thammasat School of Engineering, Thammasat University, Pathumthani 12120, Thailand*

³*Center of Excellence in Environmental Catalysis and Adsorption, Thammasat University, Pathumthani 12120, Thailand*

⁴*Engineering Product Development (EPD), Singapore University of Technology and Design, 487372, Singapore*

⁵*Environmental Research Institute, Chulalongkorn University, Bangkok 10330, Thailand*

Received: 30 June 2022/Accepted: 5 December 2022

ABSTRACT

The development of photocatalytic treatment in continuous flow systems to be more practical is challenging. This research aimed to study batch and continuous flow treatment of trichloroethylene (TCE) contaminated in water by silver and cerium doped zinc oxide (0.005Ag-0.005Ce-ZnO) visible light driven photocatalyst. This catalyst was selected to represent the green route synthesis with simplicity and ease of upscaling. The 0.005Ag-0.005Ce-ZnO powder was synthesized using sticky rice flour as a template. Mechanical coating of the 0.005Ag-0.005Ce-ZnO powder on activated alumina (Al₂O₃) beads was done to improve the appropriate packing in the fixed bed columns. Characterization of 0.005Ag-0.005Ce-ZnO showed a higher response to visible light and smaller crystallite size compared to zinc oxide synthesized with the same method. Using sticky rice starch as a template increased the uniform distribution of the elements. The photocatalytic batch test over 0.005Ag-0.005Ce-ZnO powder, 0.30 g/100 mL, could remove TCE up to 80% in 180 min. The decrease of TCE via photocatalysis compared to volatilization, adsorption, and photolysis presented the predominance of photocatalysis. Langmuir-Hinshelwood kinetics described that the decrease of TCE more depended on the reaction than adsorption. In addition, the TCE degradation steadily remained at 80-90% along the run of 0.005Ag-0.005Ce-ZnO@Al₂O₃ photocatalysis under visible light from both warm white lamps and sunlight in the continuous flow system. Besides photocatalysis, TCE adsorption on 0.005Ag-0.005Ce-ZnO@Al₂O₃ packed in the columns showed significant results. Our findings presented the possibility of applying the photocatalytic continuous flow system to remove TCE in industrial wastewater.

Keywords: Continuous flow system; fixed bed column; photocatalysis; visible light; zinc oxide

ABSTRAK

Pembangunan rawatan fotopemangkinan dalam sistem aliran berterusan untuk menjadi lebih praktikal adalah mencabar. Penyelidikan ini bertujuan untuk mengkaji kumpulan dan rawatan aliran berterusan trikloroetilena (TCE) tercemar dalam air oleh perak dan cerium terdop zink oksida (0.005Ag-0.005Ce-ZnO) pemangkinan dipacu cahaya nampak. Pemangkin ini dipilih untuk mewakili sintesis laluan hijau dengan kesederhanaan dan kemudahan peningkatan. Serbuk 0.005Ag-0.005Ce-ZnO telah disintesis menggunakan tepung beras melekit sebagai templat. Salutan mekanikal serbuk 0.005Ag-0.005Ce-ZnO pada manik alumina teraktif (Al₂O₃) telah dilakukan untuk menambah baik pembungkusan yang sesuai dalam turus lapisan tetap. Pencirian 0.005Ag-0.005Ce-ZnO menunjukkan tindak balas

yang lebih tinggi kepada cahaya boleh nampak dan saiz kristal yang lebih kecil berbanding zink oksida yang disintesis dengan kaedah yang sama. Penggunaan kanji beras pulut sebagai templat meningkatkan pengagihan unsur secara seragam. Ujian kumpulan fotopemangkinan ke atas serbuk 0.005Ag-0.005Ce-ZnO, 0.30 g/100 mL boleh mengeluarkan TCE sehingga 80% dalam 180 min. Penurunan TCE melalui fotopemangkinan berbanding dengan peruapan, penjerapan dan fotolisis menunjukkan dominasi fotopemangkinan. Kinetik Langmuir-Hinshelwood menggambarkan bahawa penurunan TCE lebih bergantung kepada tindak balas daripada penjerapan. Di samping itu, kemerosotan TCE secara berterusan kekal pada 80-90% sepanjang kajian fotopemangkinan 0.005Ag-0.005Ce-ZnO@Al₂O₃ di bawah cahaya boleh nampak daripada kedua-dua lampu putih hangat dan cahaya matahari dalam sistem aliran berterusan. Selain fotopemangkinan, penjerapan TCE pada 0.005Ag-0.005Ce-ZnO@Al₂O₃ yang terpadat dalam turus menunjukkan hasil yang ketara. Penemuan kami membentangkan kemungkinan menggunakan sistem aliran berterusan fotopemangkinan untuk menyingkirkan TCE dalam air sisa industri.

Kata kunci: Cahaya boleh nampak; fotopemangkinan; sistem aliran berterusan; turus lapisan tetap; zink oksida

INTRODUCTION

The development of photocatalysts' properties through several synthesis methods has grown rapidly and intensively over the past decades. The photocatalysts with outstanding and suitable properties are lined up for use. Research on wastewater treatment by the photocatalytic process has been very successful in the batch test system. However, the most important limitation of the photocatalytic process is that allowing the photocatalyst's surface to be properly exposed to light and targeted pollutants is difficult when scaling up the treatment system (Laudadio & Noël 2021). It means that light intensity hardly penetrates reactor diameters increased. The next thing to consider is that most of the photocatalysts are in a powder form which is not ready for environmental applications unless the photocatalysts would be modified, immobilized, pelletized, or coated on supporting materials. A continuous flow treatment system in a fixed-bed column for photocatalytic technology is the research to be done to prove the usability of efficient photocatalysts in real practices. Moreover, another challenge of photocatalytic continuous flow treatment investigation is how to enable light (photons) to activate the surface of catalysts in the reactor. Thus, transparent material, geometries of photoreactors and reflectors, cooling system, and solvent-reactor compatibility affects the performance of photocatalytic continuous flow treatment (Su et al. 2014).

Attention to ZnO modification has been paid to metal doping to enhance the visible light photocatalytic activity (Mittal et al. 2016). Ag-ZnO and Ce-ZnO has been widely studied in photocatalysis applications to degrade various pollutants such as pharmaceutical wastewater

(Hosny et al. 2022), organic dyes in water (Hu et al. 2019; Shenoy et al. 2021), and pesticides and herbicides (Veerakumar et al. 2021). However, the application of bimetal of Ag-Ce doped ZnO in trichloroethylene (TCE) degradation is not known. Based on previous findings, silver and cerium-doped zinc oxide (0.005Ag-0.005Ce-ZnO) visible light driven photocatalyst presented superior efficiency to degrade the pollutant contaminated in water (Khamdahsag et al. 2018). With cerium-doped zinc oxide (Ce-ZnO) which was prepared via a simple chemical method by using sticky rice starch as a template, increased the uniform distribution of the elements (Khamdahsag et al. 2012), the appearance of a CeO₂ at 111 plane in XRD patterns was found for all ZnO doped Ce samples. The Ce-ZnO can absorb in the ultraviolet (UV) region, as well as in the visible light range (400-800 nm) observed from UV-DR. The 0.02Ce-ZnO provided efficient removal of an organic pollutant, atrazine, at the pH of the isoelectric point. Therefore, doping transition metal such as cerium probably increases the effectiveness for visible light range absorption and plays a role in enhancing photocatalytic activity under visible light irradiation.

Subsequently, a superior photocatalytic degradation rate of Ag-Ce-ZnO was found in our study compared to Fe and Cu metal dopants (Khamdahsag et al. 2018). 0.005Ag-0.005Ce-ZnO exhibited a higher atrazine removal than 0.005Fe-0.005Ce-ZnO and 0.005Cu-0.005Ce-ZnO. The Ag-Ce-ZnO catalyst showed high photocatalytic activity due to the higher absorption in the range of visible light (Pongwan et al. 2012). The activity may be from a synergistic effect between silver and Ce⁴⁺ to trap electrons with its subsequent transfer to the adsorbed oxygen (Kumar & Rao 2015). The efficiency

of 0.005Ag-0.005Ce-ZnO suggests a possibility for the application under sunlight.

UV-DR measurement can provide the response of UV and visible light absorption of the catalyst. Two absorption peaks at 368 and 450 nm of Ag/ZnO were observed (Liu et al. 2015). The broadening and intensity of the peak at 450 nm increased with increasing Ag doping. The absorption peak at 450 nm was the characteristic plasmon absorption of Ag nanoparticles in Ag/ZnO and was red-shifted, compared to pure Ag ones, due to strong interfacial electronic coupling between Ag and ZnO.

Ag could grant surface plasmon resonance (SPR), while Ce has oxygen vacancies. They are also stable in cubic metal form in the case of Ag and metal oxide form in the case of Ce. Prominently, these dopants present high photocatalytic activity together with ZnO. However, the ratio of doping is one of the important parameters. The photocatalytic mechanism of Ag/ZnO under UV and visible light irradiation was reported (Liu et al. 2015). Through rational design, Ag/ZnO can effectively utilize UV light in the solar spectrum to generate charge carriers for photocatalytic reactions, whereas the visible light in the solar spectrum can be synergically used for SPR excitation to enhance the charge separation and photocatalytic efficiency.

Therefore, this study was objected to study batch and continuous flow treatment of representing pollutant probe, TCE, contaminated in water by silver and cerium doped zinc oxide (0.005Ag-0.005Ce-ZnO) visible light driven photocatalyst. Along with the synthesis, green chemistry principles were applied. Characterization techniques were tested to understand the physic-chemical properties of the Ag and Ce doped ZnO catalyst. The experimental parameters, including catalyst loading, pH, and initial concentration of TCE were studied in a batch treatment system. The blank tests of volatilization, adsorption, and photolysis of TCE were investigated. A continuous flow treatment system in a fixed bed photoreactor for photocatalytic degradation of TCE under different visible light sources was reported.

MATERIALS AND METHODS

SYNTHESIS OF 0.005Ag-0.005Ce-ZnO POWDER

This synthetic method was based on the previous reports (Khamdahsag et al. 2018, 2012). Metal salts of zinc nitrate hexahydrate (Acros Organics, 98%), cerium nitrate hexahydrate (Acros Organics, 99.5%), and silver nitrate (Carlo Erba Reagents, 99.8%), were used as Zn, Ce, and Ag sources in the synthesis of molar ratio

catalyst 0.005Ag-0.005Ce-ZnO. Through the green route synthesis, sticky rice flour (Erawan, Thailand) was used as a polymeric natural template to support and uniformly disperse Zn, Ce, and Ag ions during the synthesis. Deionized water was used as a solvent for preparing the metal salt solution and the sticky rice flour gel. The weight ratio of zinc nitrate hexahydrate to sticky rice flour was controlled at 5:1 by weight. Initially, sticky rice flour mixed with 200 mL of deionized water was stirred and cooked at 80 °C for 30 min to obtain the sticky rice flour gel. After that, each 20 mL of zinc nitrate, cerium nitrate, and silver nitrate solution was added to the sticky rice flour gel. The mixture was stirred and heated to 80 °C for another 30 min before drying in an oven at 100 °C for 48 h. The resulting solids from the oven were then calcined at 550 °C for 3 h using a heating rate of 2 °C/min. Finally, the 0.005Ag-0.005Ce-ZnO catalyst was obtained apparently as a light gray color. The catalyst was ground and sieved in size of less than 0.15 mm.

PREPARATION OF 0.005Ag-0.005Ce-ZnO@Al₂O₃

The 0.005Ag-0.005Ce-ZnO catalyst powder was adhered to the surface of activated alumina (Al₂O₃) beads using the mechanical coating technique. The weight ratio of the 0.005Ag-0.005Ce-ZnO powder to activated alumina beads was 12:120. Initially, the activated alumina beads in diameter of 0.5-1.2 mm (Pingxiang Huihua Packing, China) was introduced into a stainless-steel milling pot. Then, little water was sprayed on the activated alumina beads to moisturize them and make them ready to be adhered by the 0.005Ag-0.005Ce-ZnO powder on their surface. The two solid mixtures were swirled at 300 rpm for 15 h. Then, activated alumina beads with 0.005Ag-0.005Ce-ZnO adhesion, so-called 0.005Ag-0.005Ce-ZnO@Al₂O₃, were poured out from a stainless-steel milling pot and sieved to remove the remaining catalyst powder. Only the 0.005Ag-0.005Ce-ZnO@Al₂O₃ portion was calcined at 550 °C at a heating rate of 2 °C/min for 24 h. Then, the 0.005Ag-0.005Ce-ZnO@Al₂O₃ was ready to use with approximately 7.7% of 0.005Ag-0.005Ce-ZnO powder adhered on 0.005Ag-0.005Ce-ZnO@Al₂O₃.

CHARACTERIZATION OF PHOTOCATALYST X-RAY DIFFRACTION

The crystal structure of the catalyst powders was analyzed using Bruker D8 Advance (Germany) x-ray diffractometer (XRD) using a Cu K α source ($\lambda = 0.15406$ nm) with a Lynx Eye detector. The samples were scanned

in the 2θ range of 20-80°, accelerating voltage of 40 kV, emission current of 40 mA, time record of 0.5 s, increment of 0.05°, and effective time of 627.5 s. The crystallite size of the catalysts was calculated from the Debye-Scherrer equation (Wang et al. 2009, 2008).

UV-vis DIFFUSIVE REFLECTANCE ABSORPTION

The absorbance of the catalyst powders was obtained using HITACHI U-3501 (Japan) UV-vis spectrophotometer. The data obtained from this instrument were the UV-vis diffusive reflectance absorption (UV-DR). 2 g of dry catalyst powders were lightly pressed into a thin flat circle mold and closed with quartz to smoothen the surface of the catalyst powders. The mold was then inserted into the UV-vis spectrophotometer containing deuterium and halogen lamps as the light sources. Barium sulfate powder was used as a reference sample to make the baseline. The spectra were recorded in the 300-800 nm wavelength range. The data was plotted between the wavelength and the absorbance curve.

N₂ ADSORPTION-DESORPTION

The specific surface area of the catalyst powders was obtained by testing with Quantachrome Instrument Autosorb-1 (USA) nitrogen adsorption apparatus. Before the experiment, 0.1000-0.3000 g of the catalysts was degassed at 150 °C for 1-2 h to remove moisture and various volatile substances. The catalyst was tested for nitrogen adsorption at -196 °C. Brunauer-Emmett-Teller (BET) method was applied to calculate the surface area.

ELECTRON MICROSCOPY ANALYSES

The morphology of the catalyst powders was analyzed by using JEOL JSM-6400 (Japan) scanning electron microscopes with energy dispersive X-ray analysis (SEM/EDX) using 3000-time magnification. Firstly, the catalysts were dried at 100 °C for 48 h and then sprinkled onto a round iron stub with carbon tape. In this analysis, the catalyst samples were not gold-plated because they have semi-conductor properties. Finally, the stub was brought into the SEM/EDX for surface characterization and distribution of the elements that complied with the catalysts. The morphology of the catalyst powders was also analyzed by JEOL JEM-2100 (Japan) transmission electron microscopy with energy-dispersive X-ray spectroscopy (TEM/EDX).

ZETA POTENTIOMETRY

Zeta potentiometry is an analysis to understand the

surface charge properties of the catalyst powders and to determine the isoelectric point (IEP). Before the analysis, the deionized water was pH adjusted by 0.25-M hydrochloric acid and 0.25-M sodium hydroxide solution to obtain the adjusted solution at pH 2-12. 5.0 mg of catalysts were then immersed in 20 mL of the pH-adjusted solution and shaken for 24 h. The analysis was performed using MALVERN Instruments nanoseries (France) zetasizer using a refractive index of ZnO at 2.008. The catalysts suspended in the pH-adjusted solution were then introduced to the measurement cell. The analysis was performed in triplication with a maximum of 30 repetitions of automatic counting. The obtained values were plotted between zeta potential (mV) and pH. The particle size of catalysts was analyzed by the zetasizer. The analysis was done in 5 replications. The instrument reported the number of particle size counts found in the sample.

PHOTOCATALYTIC DEGRADATION TEST

BATCH TREATMENT SYSTEM

The photocatalytic degradation in a batch system was done at a temperature of 25±1 °C controlled by cooling water circulation. 100 mL of TCE solution at different concentrations and catalyst powder at different weights were prepared. Then, they were introduced into a 250 mL flask capped with a glass stopper. The flask was put into the batch reactor with the light off and stirred using a magnetic stirrer immediately, as well as the timer started. After the TCE solution and catalyst were subjected to dark conditions for 30 min, the TCE photocatalytic degradation reaction was initiated by turning on warm white light (4 lamps, Philips E27 100W). The average visible light intensity in the reactor was 760.75 W/m² measured by Kimo SL100 (France) solarimeter. In addition, the average UV light intensity in the reactor was 0.00 mW/cm² measured by a 5.0 digital (USA) UV meter. Samples were collected with a volume of 2 mL using syringes. The 1 mL sample was then discarded by a filter (PTFE syringe filter, 0.45 μm, Ø = 13 mm). The remaining 1 mL sample was filtered and ready for TCE concentration analysis. All results were calculated using the average value obtained from the replication testing.

In the experimental design, fundamental factors that may influence the catalyst's ability to degrade TCE were studied, including the catalyst loading, the effect of pH in TCE solution, the initial concentration of TCE solution, and the rate of the reaction. The photocatalytic experiment compared the disappearance of TCE with the evaporation, adsorption, and photolysis reactions of the TCE solution.

CONTINUOUS FLOW TREATMENT SYSTEM IN FIXED BED PHOTOREACTOR

In a continuous flow treatment system, 100 mg/L TCE solution was prepared for 40-100 L in 20 L gallon without pH adjustment (pH 6). The fixed bed photoreactor operated at a temperature of 32 ± 2 °C, heated by light sources. Firstly, three sets of 7.0000 g of 0.005Ag-0.005Ce-ZnO@Al₂O₃ prepared by mechanical coating technique were packed 15 cm in length into three hollow borosilicate glass columns, an inner diameter of 1 cm, covered with cotton wool at the top and bottom. The center of the columns was inserted with a glass rod, a diameter of 0.5 cm and 15 cm long, to reduce the amount of 0.005Ag-0.005Ce-ZnO@Al₂O₃ used to fill the column at a central position where they were not exposed to light. Thus, a reactor with an annular-like column was created. Mirror and aluminum foil were used as reflectors placed under and sides of the columns. The silicone tubes were then connected in series with the three columns and arranged as in Figure 1. The photocatalyst test for TCE degradation was conducted under 2 different visible light sources, artificial light from warm white lamps and sunlight.

In experiments under visible light of warm white lamps (1 lamp, Philips E27 100W), the TCE solution (100 mg/L) was pumped at a flow rate of 60 mL/min through the columns containing 0.005Ag-0.005Ce-ZnO@Al₂O₃ in dark conditions to trace the disappearance of TCE in solution via adsorption process. When the concentration of the TCE solution became constant, then the lights were on. The average visible light intensity in the reactor was 601.67 W/m², and the average UV light intensity in the reactor was 0.00 mW/cm². The samples were collected under the method as same as they were done in the batch treatment system.

The experiment under sunlight was conducted from 8:20 am to 5:35 pm on a sunny day. The TCE solution (100 mg/L) was pumped through the columns containing 0.005Ag-0.005Ce-ZnO@Al₂O₃ under the flow rate of 60 mL/min. Visible light intensity was measured by the solarimeter and UV light intensity was measured by the UV meter. Light intensity was measured consistently at the time of sample collection. The method of sampling and analysis was the same as for the experiment under the visible light of warm white lamps.

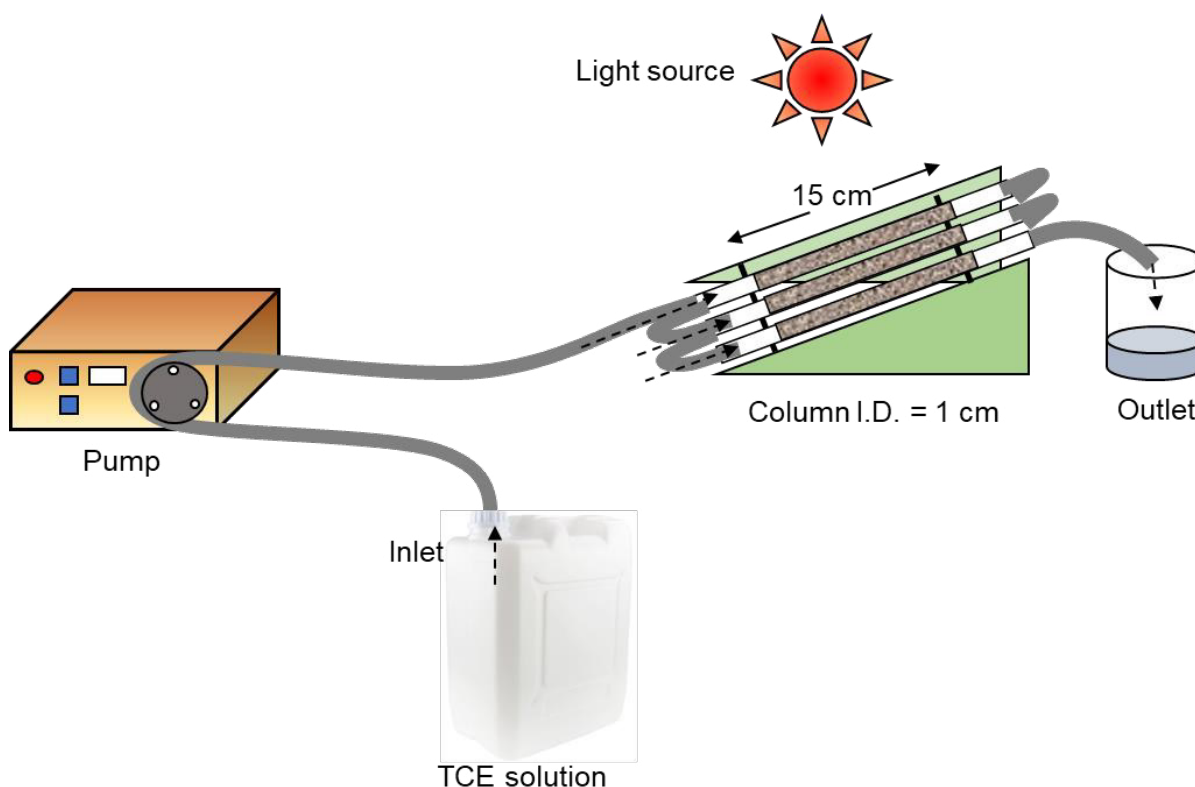


FIGURE 1. Fixed bed photoreactor setup for continuous flow treatment of TCE over 0.005Ag-0.005Ce-ZnO@Al₂O₃

ANALYSIS OF TCE CONCENTRATION

The concentration of TCE solution was analyzed using Agilent Technologies (USA) high-performance liquid chromatography (HPLC). HPLC condition setup in this experiment was based on research by Kim et al. (2007) using Hypersil C18 ODS column of 4.0×125 mm, 5 μm, and column temperature of 35 °C. The column was connected to HPLC-DAD 1200 diode-array detector and a pump with the regulator. The UV absorbance was set to 214 nm to measure the maximum amount of TCE absorbance. The mobile phases were acetonitrile and water at a ratio of 85:15 with a flow rate of 1.0 mL/min. Before analysis, the mobile phases were filtered and degassed for 60 min. The injected sample volume was 50 μL and the analysis took 8 min/sample. The concentration of the TCE solution was calculated from the equation obtained from the calibration curve.

RESULTS AND DISCUSSION

CHARACTERISTICS OF 0.005Ag-0.005Ce-ZnO

To access physical and chemical properties, we characterized the synthesized 0.005Ag-0.005Ce-ZnO by XRD, UV-DR, zeta potentiometry, N₂ adsorption-desorption, SEM-EDX, and TEM.

The XRD pattern of 0.005Ag-0.005Ce-ZnO confirmed the characteristic peak of ZnO at (100), (002), (101), (102), (110), (103), (112), and (201) planes (Figure 2(A)), indicating the structure of Wurtzite ZnO (JCPDS, 36-1451), corresponding to previous studies (Liang et al. 2019; Wu, Li & Li 2019). We did not observe characteristic XRD peaks of Ag and Ce. It might be that the amount and particle size of doped Ag and Ce were too small. Thus, XRD could not detect Ag and Ce clearly, which corresponded to previous studies (Pavithra & Jessie Raj 2022; Sukriti et al. 2020). The average crystallite size of 0.005Ag-0.005Ce-ZnO was calculated by the Debye-Scherrer equation in (1) (Khanchandani et al. 2014);

$$D_{\text{XRD}} = 0.9 \lambda / \beta \cos \theta \quad (1)$$

where D_{XRD} is the average crystallite size; λ is the wavelength of Cu K α 0.15406 nm; β is the width at half maximum (FWHM) of characteristic XRD peaks; and θ is the angle (degree). The synthesized 0.005Ag-0.005Ce-ZnO had an average crystallite size of 31.56 nm.

To elucidate the effect of doped Ag and Ce on ZnO to the light absorption, we measured 0.005Ag-0.005Ce-ZnO by UV-DR in the wavelength of 300-800 nm. In

Figure 2(B), the ZnO showed the absorption edge (λ_g) in the UV range at 340 nm, corresponding to previous studies (Akhtar et al. 2020; Pudukudy & Yaakob 2015). The doped 0.005Ag-0.005Ce on ZnO shifted the absorbance towards a higher wavelength (380-700 nm). Moreover, there was no red shift on 0.005Ag-0.005Ce-ZnO compared to ZnO, indicating no change in the gap energy of ZnO. These results suggested that 0.005Ag-0.005Ce doping into the ZnO lattice extended the working wavelength for photocatalysts, which showed a potential to use as a photocatalyst for TCE degradation at visible light.

To elucidate the effect of doped Ag and Ce on ZnO to surface charge, we analyzed the change of surface charge at various pH (2-12) solutions by zeta potentiometry (Figure 2(C)). ZnO showed an IEP at pH 8.6, similar to a previous study (Miao et al. 2014). ZnO showed a positive charge at low pH than the IEP and a negative charge at high pH than the IEP. The presence of Ag and Ce on ZnO led to a change in surface charge. 0.005Ag-0.005Ce-ZnO showed a positive charge at pH 2, whereas it showed a negative charge at pH 6-8 and the IEP at pH 4 and 10-12. These results indicated that the presence of Ag and Ce on ZnO shifted the surface charge of ZnO and the IEP at higher pH. Additionally, the zetasizer analysis of 0.005Ag-0.005Ce-ZnO showed the average particle size of 936.1 nm.

To determine the change in surface area, we analyzed 0.005Ag-0.005Ce-ZnO by N₂ adsorption-desorption. The specific surface area was calculated based on Brunauer-Emmett-Teller (BET) model. The specific surface area slightly increased from 7 to 17 m²/g after Ag and Ce doping. This result suggested an increase in the surface was due to a reduction in the crystallite size of ZnO after Ag and Ce doping, corresponding to crystallite size results calculated from XRD spectra (Figure 2(D)).

To elucidate the morphology of catalysts, we analyzed SEM and TEM on 0.005Ag-0.005Ce-ZnO. SEM image of 0.005Ag-0.005Ce-ZnO showed porous catalyst particles due to the use of sticky rice starch as a template during synthesis (Figure 3(A)). Moreover, we observed an aggregation of catalyst particles due to van der Waals attraction between particles. To access the homogeneity of Ag and Ce doped on ZnO, we analyzed elemental mapping by EDX spectroscopy. Elemental mapping showed that cerium, zinc, and oxygen were well dispersed, indicating homogenous synthesis (Figure 3(B)-3(D)). However, we did not observe silver elemental. It might be that an amount of silver was too low to be detected by EDX spectroscopy. Moreover, TEM images showed the morphology of 0.005Ag-0.005Ce-

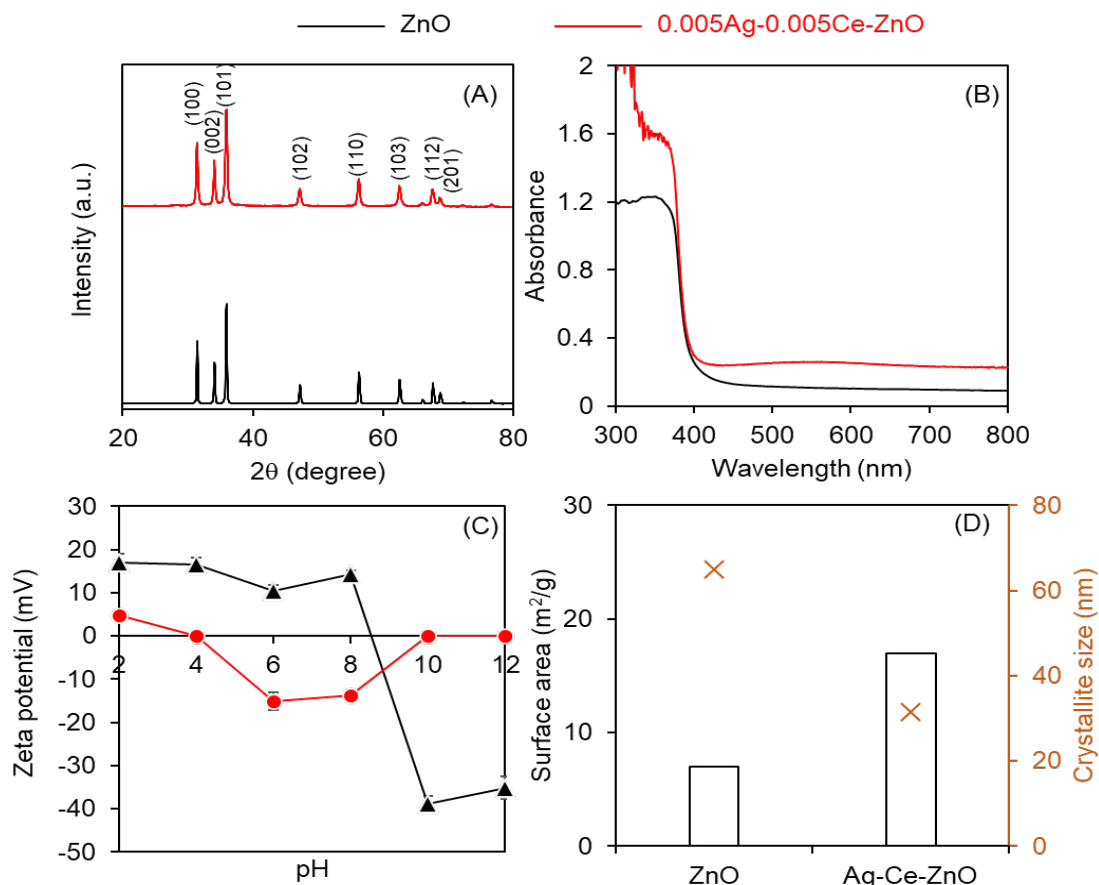


FIGURE 2. Characterization of ZnO and 0.005Ag-0.005Ce-ZnO, (A) XRD profiles, (B) UV-DR, (C) zeta potentiometry, and (D) BET specific surface area calculated from N_2 adsorption-desorption and crystallite size calculated from XRD patterns

ZnO particles in spheres with a grain size of about 20-50 nm, which is also confirmed by the crystallite size calculated from the XRD result (Figure 3(E)-3(F)). The measured lattice spacing of 0.24, 0.28, and 0.31 could be attributed to the (111) plane of Ag and (104) plane of CeO_2 , (111) plane of ZnO, and (112) plane of CeO_2 , respectively. Thus, the results confirmed the formation of Ag and Ce doped on the ZnO surface.

PHOTOCATALYTIC PERFORMANCE BATCH TREATMENT SYSTEM

To test the photocatalytic performance of 0.005Ag-0.005Ce-ZnO, we tested the degradation of TCE under visible light. As a control, ZnO showed about 63% TCE degradation at 30 min and kept constant at 39% TCE degradation under visible light (Figure 4(A)). Compared to 0.005Ag-0.005Ce-ZnO, TCE degradation was 54% at 30 min. An increase in reaction time improved TCE degradation from 54 to 73% within 180 min (Figure

4(A)). This result suggested that the doped Ag and Ce on ZnO surface promoted photocatalytic activity.

TCE is a volatile organic solvent with low vapor pressure. Various parameters such as TCE vaporization, TCE adsorption, and TCE degradation by visible light may cause the misleading photocatalytic performance of 0.005Ag-0.005Ce-ZnO. To decouple the effect of those parameters, we tested (1) TCE removal by volatilization without visible light and catalyst, (2) TCE removal by photolysis without catalyst, and (3) TCE removal by adsorption on catalyst without visible light (Figure 4(B)). Although TCE could be removed by TCE volatilization, photolysis, and adsorption on the catalyst, photocatalysis could potentially improve TCE removal under visible light. TCE removal by volatilization, photolysis, and adsorption was 40% at 30 min. An increase in reaction time slightly improved TCE removal by 43-50% at 180 min. Among volatilization, photolysis, and adsorption, the volatilization process played an important role in TCE

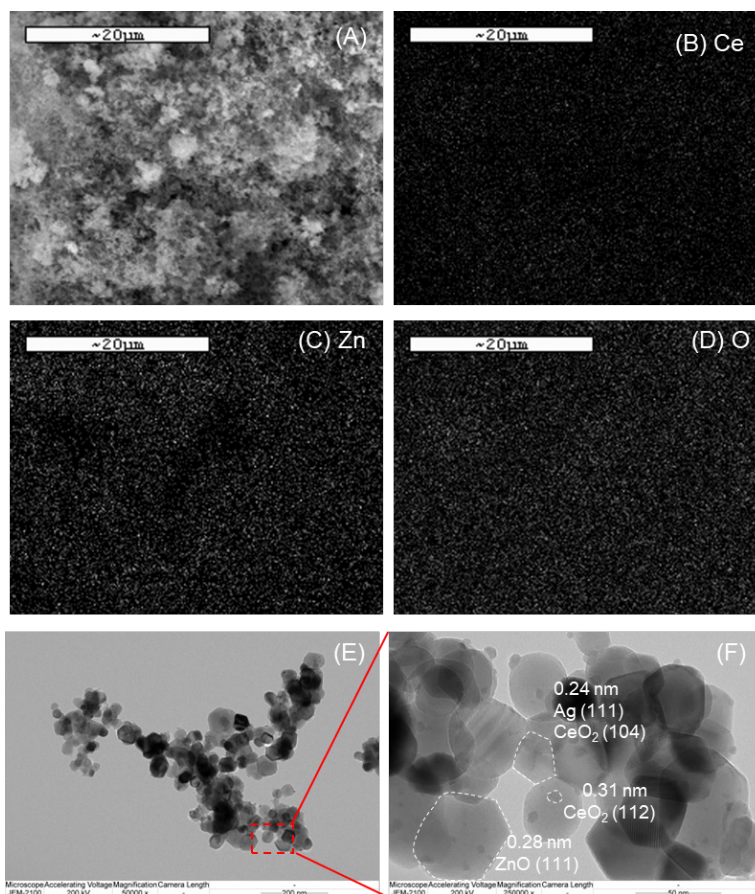


FIGURE 3. (A) SEM image of 0.005Ag-0.005Ce-ZnO with elemental mapping of (B) Ce, (C) Zn, and (D) O, and (E-F) TEM images

removal from the batch system. Photolysis and adsorption showed a slight drop in efficiency to the volatilization process. Compared to photocatalysis of 0.005Ag-

0.005Ce-ZnO, TCE was removed to 54% at 30 min and progressively dropped to 73% at 180 min. These results suggested that photocatalysis improved TCE removal.

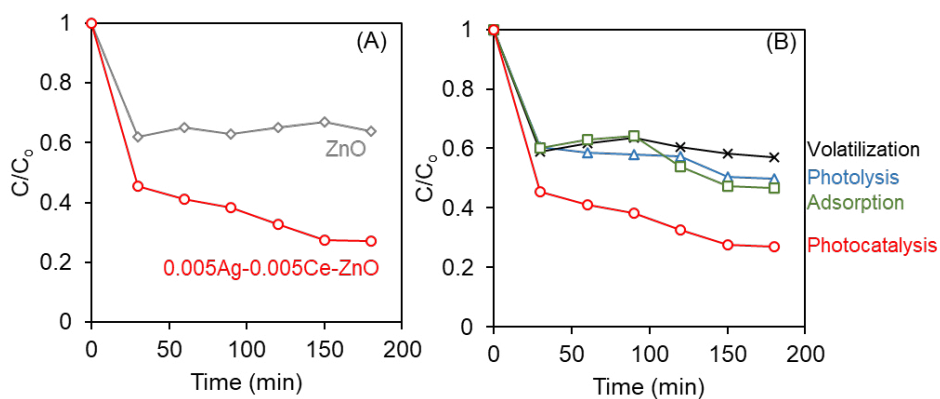


FIGURE 4. (A) Photocatalytic performance of ZnO and 0.005Ag-0.005Ce-ZnO under visible light and (B) control experiments of 0.005Ag-0.005Ce-ZnO (experimental conditions: 100 mg TCE/L, 1 g catalyst/L, and pH 6)

To elucidate the effect of catalyst loading, initial pH, and TCE concentration on the photocatalytic performance of 0.005Ag-0.005Ce-ZnO, we performed parameter studies in a batch reactor. First, catalyst loading was varied from 0.05 to 0.3 g/100 mL TCE solution (88.9 mg/L) with a constant of initial pH at 6. An increase in catalyst loading from 0.05 g/100 mL to 0.3 g/100 mL improved TCE removal from 60 to 73% at 180 min (Figure 5(A)). These results suggested that a low amount of catalysts caused a lack of active catalytic sites to produce oxidative species to degrade TCE. In contrast, a high amount of catalyst might cause a cloudy solution that shields visible light to act on the catalyst surface, leading to a drop in catalytic performance. Thus, we selected a catalyst at 0.3 g/100 mL to study further. Second, we studied the effect of initial pH by variation

of pH in a range of 2-11 (Figure 5(B)). The natural pH of a solution at pH 6, in which the TCE solution was prepared using deionized water as a solvent without pH adjustment, showed TCE removal of 65%. An increase in pH from 2 to 11 improved TCE removal from 60 to 81%. These results suggested that a basic condition promoted TCE degradation. An increase in pH improved OH⁻ concentration. The OH⁻ could be oxidized further by the hole to OH radicals. Thus, the basic solution could promote the photocatalytic performance of 0.005Ag-0.005Ce-ZnO (Miao et al. 2014). The surface charge of 0.005Ag-0.005Ce-ZnO, which was normally associated with the adsorption step of pollutants on the catalyst surface before the degradation reaction step occurred, was likely to be insignificant in this case compared to the OH⁻ from the pH solution increase. However, the natural

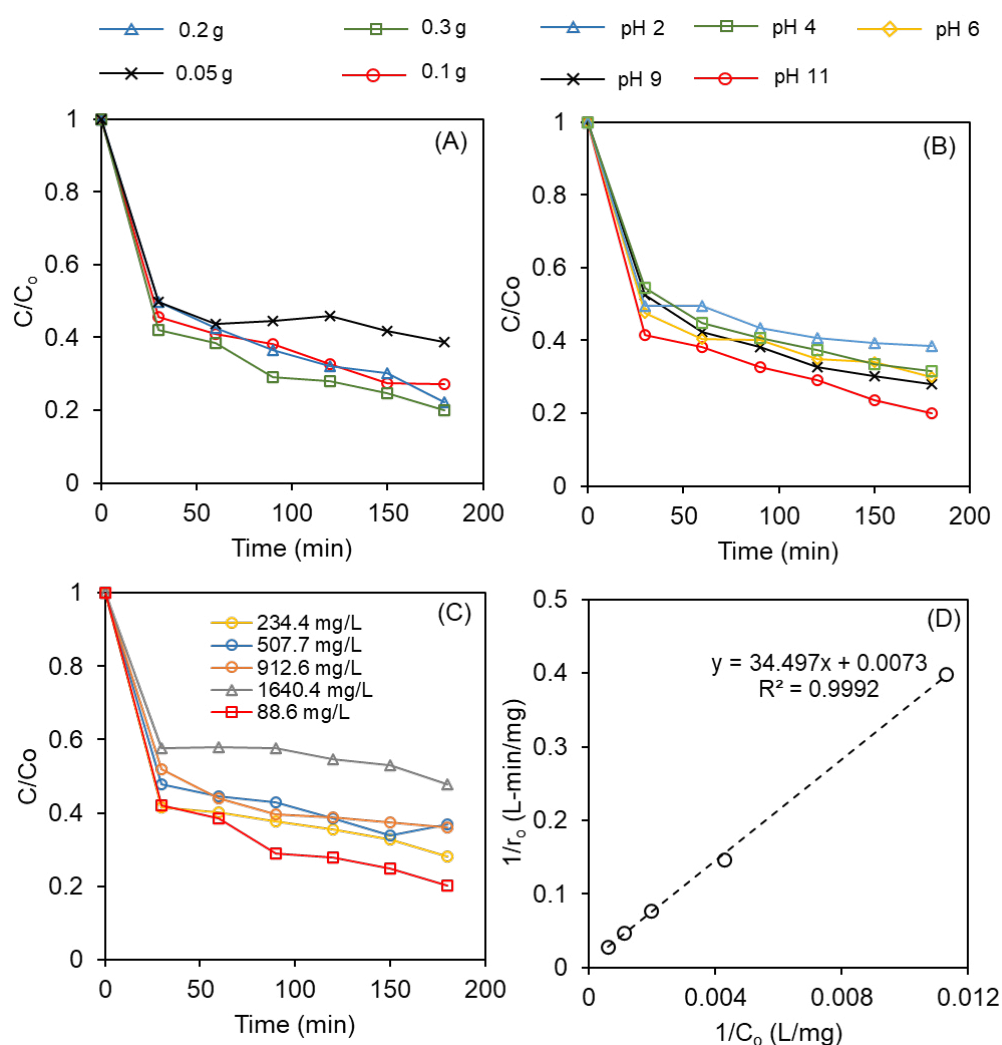


FIGURE 5. Parameter studies of 0.005Ag-0.005Ce-ZnO photocatalysis (A) effect of catalyst loading, (B) effect of initial pH, (C) effect of TCE concentration, and (D) Langmuir-Hinshelwood linear plot (experimental conditions: 88.6-1640.4 mg TCE/L, 0.05-0.3 g catalyst/100 mL, and initial pH 2-11)

pH solution also gave high TCE removal (65%). To avoid operating costs and many steps, we selected natural pH solution (pH 6) to study further.

Lastly, we studied the effect of TCE concentration by variation of TCE concentration from 88.6 to 1640.4 mg/L (Figure 5(C)). An increase in TCE concentration from 88.6 to 1640.4 mg/L decreased TCE removal from 80 to 50%. These results suggested that photocatalytic performance strongly depended on the amount of TCE to catalyst active sites. High TCE concentration caused a lack of catalyst active sites to decompose TCE.

To compare the photocatalytic degradation efficiency of Ag and Ce doped on ZnO, we summarized previous studies in Table 1. Ce doped on ZnO improved rhodamine B degradation by up to 98% in 120 min (Hu et al. 2019). Ag doped on ZnO@Biochar degraded tetracycline up to 70% at 60 min (Hosny et al. 2022). Our previous study found that Ag and Ce doped on ZnO could enhance photocatalytic degradation of atrazine up to 82% at 120 min. Furthermore, bimetallic Ag and Ce doped on ZnO showed high TCE degradation of 81% at 180 min in this study. This result suggested that Ag and Ce doped on ZnO was promising catalyst for photocatalytic degradation.

TABLE 1. Comparison of photocatalytic degradation efficiency of Ag and/or Ce doped on ZnO-based photocatalyst reported in literature

Photocatalyst	Pollutant concentration	Experimental condition	Efficiency	Reference
<u>Batch system</u>				
Ce-ZnO	Rhodamine B, 10 mg/L	catalyst loading = 0.7 g/L, pH 9.0, T = 50°C	98%, 120 min	Hu et al. (2019)
Ag-ZnO@Biochar	Tetracycline, 50 mg/L	catalyst loading = 0.5 g/L, pH 6.0, T = 25°C, H ₂ O ₂ = 100 mM	70%, 60 min	Hosny et al. (2022)
0.005Ag-0.005Ce-ZnO	Atrazine, 5 mg/L	catalyst loading = 1 g/L, pH 0.9, T = 25°C, visible light	82%, 120 min	Khamdahsag et al. (2018)
0.005Ag-0.005Ce-ZnO	TCE, 100 mg/L	catalyst loading = 3 g/L, pH 11.0, T = 25°C, visible light	81%, 180 min	This study

Based on the effect of the initial concentration of TCE on the photocatalysis reaction, the initial reaction rate (r_0) can be calculated from (2) (Fogler 2006);

$$r_0 = ((-3C_0 + 4C_1 - C_2) / 2\Delta t) \quad (2)$$

where r_0 is an initial photocatalytic degradation rate (mg/L-min); C is a concentration of TCE at reaction time t (mg/L); and Δt is $t_2 - t_1$ (min). Subsequently, the r_0 values can be calculated to determine the relationship between the initial TCE degradation rates and the initial TCE concentration (C_0) using the linear equation of Langmuir-Hinshelwood (3);

$$r_0 = (k_r K_{ads} C_0) / (1 + K_{ads}) \quad (3)$$

where k_r is the reaction rate constant (mg/L-min); K_{ads} is the adsorption equilibrium constant (L/mg); and C_0 is the initial equilibrium concentration of TCE (mg/L). The photocatalysis of TCE by 0.005Ag-0.005Ce-ZnO powder under visible light fitted well with Langmuir-Hinshelwood kinetics. A linear equation plotted between $(1/r_0)$ and $(1/C_0)$ as shown in Figure 5(D) gave the reaction constant (k_r) at 136.99 mg/L-min and the adsorption equilibrium constant (K_{ads}) at 2.12×10^{-4} L/mg. Comparing the effects of reaction and adsorption, it was found that the K_{ads} value was very small compared to k_r describing that the absence of TCE was largely dependent on the reaction effect.

CONTINUOUS FLOW TREATMENT SYSTEM IN FIXED BED PHOTOREACTOR

Previous studies demonstrated photocatalytic degradation

of TCE in various catalysts such as titanium dioxide (TiO_2), Cu/TiO_2 , and Ag/TiO_2 in the gas phase (Maldonado et al. 2010; Martnez Vargas et al. 2015; Wang et al. 2002). However, the photocatalytic degradation of TCE was not well understood in the aqueous phase. Therefore, this study may be considered one of the first works reported in the aqueous phase. To test the photocatalytic performance of 0.005Ag-0.005Ce-ZnO in a continuous process, we performed a packed bed photoreactor. 0.005Ag-0.005Ce-ZnO was a very small particle. Direct use of 0.005Ag-0.005Ce-ZnO may cause clogging in a pack bed photoreactor. Thus, we mechanically coated 0.005Ag-0.005Ce-ZnO onto Al_2O_3 spheres (Figure 6(A)). We selected Al_2O_3 spheres due to their inexpensive and inert photocatalysis. 0.005Ag-0.005Ce-ZnO@ Al_2O_3 was packed into three columns with 1 cm ID (Figure 6(B)). The center of the columns was inserted with a glass rod, a diameter of 0.5 cm and 15 cm long, to reduce the amount of 0.005Ag-0.005Ce-ZnO beads used to fill the column at a central position where they were not exposed to light. Therefore, the working volume was determined to be 26.52 mL by subtracting the volume of a glass rod from the volume of the column. When the working volume was divided by the TCE flow rate, the retention time was calculated to be 26.52 s. Then, we

tested 0.005Ag-0.005Ce-ZnO@ Al_2O_3 in dark and visible light. As a control, Al_2O_3 alone could remove TCE by about 10%. There was no significant difference under dark and visible light on TCE removal. This result suggested that Al_2O_3 was inert to photocatalysis. Under the dark condition, 0.005Ag-0.005Ce-ZnO@ Al_2O_3 showed 78% TCE removal at 30 min and slightly dropped to 75% TCE removal after 400 min (Figure 6(C)). This result suggested that 0.005Ag-0.005Ce-ZnO@ Al_2O_3 could adsorb TCE in the solution. However, TCE removal might be affected by the volatilization of TCE, similar to the batch result. Another factor that probably contributed to the decrease of TCE by volatilization during the test was the higher temperature of photoreactor ($32 \pm 2^\circ\text{C}$), which was heated by light sources compared to the temperature-controlled ($25 \pm 1^\circ\text{C}$) batch system. Under visible light, we observed a sudden increase in TCE removal from 75 to 87%. An increase in visible light exposure time remained TCE removal at 80-87%. Thus, 0.005Ag-0.005Ce-ZnO@ Al_2O_3 was active under visible light in a continuous process.

To demonstrate the application of 0.005Ag-0.005Ce-ZnO@ Al_2O_3 under sunlight (Figure 6(D)), we performed a pack bed photoreactor using sunlight from 8:20 am to 5:35 pm. We measured the intensity of visible and UV light during the experiment. At 08.30

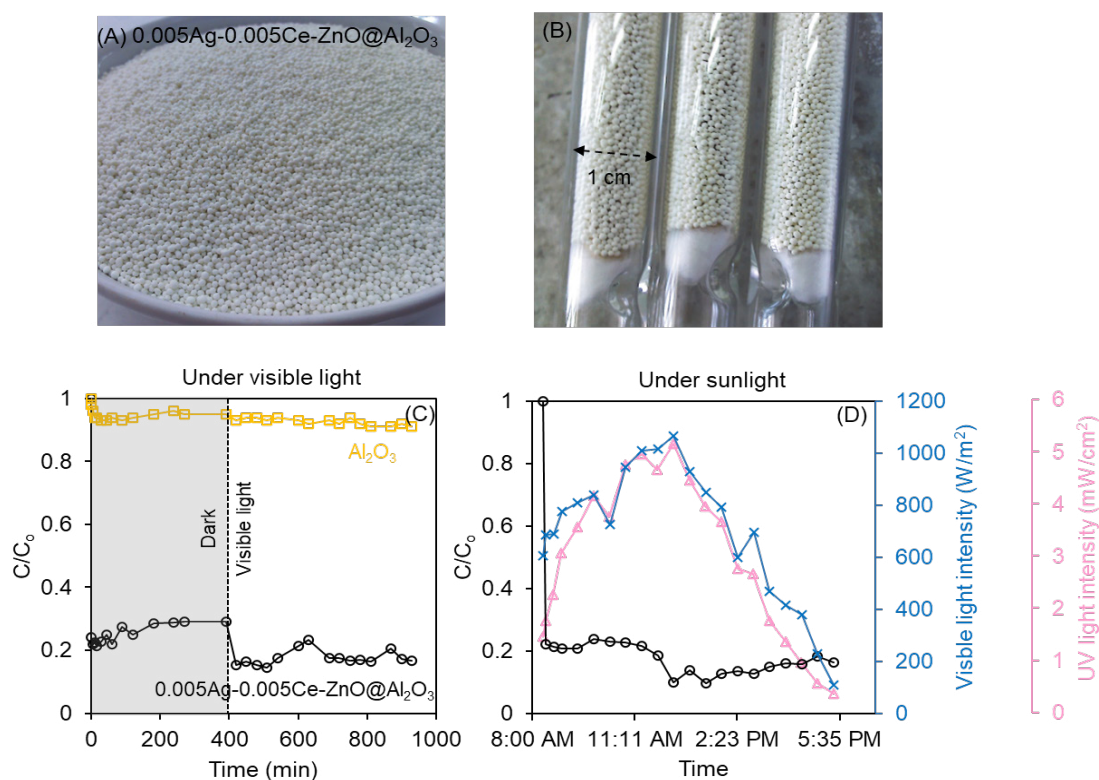


FIGURE 6. (A) Photograph of 0.005Ag-0.005Ce-ZnO coated on Al_2O_3 , (B) 0.005Ag-0.005Ce-ZnO@ Al_2O_3 in a packed column, and photocatalytic performance on 0.005Ag-0.005Ce-ZnO@ Al_2O_3 under (C) visible light and (D) sunlight (experimental conditions: 100 mg TCE/L, pH 6, and flow rate of 60 mL/min)

AM, 0.005Ag-0.005Ce-ZnO@Al₂O₃ showed 78% TCE removal. The TCE removal was increased to 90% at noon, according to the visible and UV intensities increased and maximized at noon. A decrease in visible and UV intensity caused a drop in TCE removal (About 10%). These results suggested that the application of 0.005Ag-0.005Ce-ZnO@Al₂O₃ in a packed bed photoreactor can be extended to use under sunlight. However, catalytic deactivation and catalyst recycling should be studied in the future to make this process economical.

CONCLUSIONS

The photocatalyst test in the batch treatment system for TCE degradation was compared to volatilization, adsorption, and photolysis reaction. It was found that the effect of photocatalytic degradation was greater among the others. The suitable catalyst loading was 0.3 g/100 mL in the pH range of 4-11 and TCE concentration of 88.6-234.4 mg/L. The degradation percentage of TCE decreased as the initial TCE concentration increased. Besides, the removal of TCE mainly depended on the reaction pathway rather than the adsorption one proven by Langmuir-Hinshelwood kinetics. The continuous flow treatment system in 0.005Ag-0.005Ce-ZnO beads fixed bed photoreactor showed that TCE was rapidly absorbed under dark conditions at 75% and removed up to 80-90% through the run under visible light from the lamps and sunlight implying the practicability and upscaled readiness to treat TCE in industrial wastewater.

ACKNOWLEDGEMENTS

This research was supported by Research Grant for New Scholar Ratchadaphiseksomphot Endowment Fund, Chulalongkorn University, Thailand, under Grant number: RGN_2559_029_02_54.

REFERENCES

- Akhtar, J., Tahir, A.K., Sagir, M. & Bamuffeh, H.S. 2020. Improved photocatalytic performance of Gd and Nd co-doped ZnO nanorods for the degradation of methylene blue. *Ceramics International* 46: 11955-11961.
- Fogler, H.S. 2006. *Elements of Chemical Reaction Engineering*. 4th ed. Upper Saddle River: Pearson Education, Inc.
- Hosny, M., Fawzy, M. & Eltaweil, A.S. 2022. Green synthesis of bimetallic Ag/ZnO@Biohar nanocomposite for photocatalytic degradation of tetracycline, antibacterial and antioxidant activities. *Scientific Reports* 12(1): 7316.
- Hu, B., Sun, Q., Zuo, C., Pei, Y., Yang, S., Zheng, H. & Liu, F. 2019. A highly efficient porous rod-like Ce-doped ZnO photocatalyst for the degradation of dye contaminants in water. *Beilstein Journal of Nanotechnology* 10: 1157-1165.
- Khamdahsag, P., Pimpha, N., Thongruang, R., Grisdanurak, N., Nanny, M.A. & Wittayakun, J. 2018. Photocatalysis of atrazine using ZnO texturally modified with sticky rice starch template and doped with transition metals. *Environmental Engineering and Management Journal* 17(12): 2923-2931.
- Khamdahsag, P., Pattanasiriwisawa, W., Nanny, M.A. & Grisdanurak, N. 2012. Comparative study of sticky rice starch and polyvinylpyrrolidone as templates for ZnO and Ce-ZnO synthesis. *Environmental Engineering and Management Journal* 11(4): 759-766.
- Khanchandani, S., Srivastava, P.K., Kumar, S., Ghosh, S. & Ganguli, A.K. 2014. Band gap engineering of ZnO using core/shell morphology with environmentally benign Ag₂S sensitizer for efficient light harvesting and enhanced visible-light photocatalysis. *Inorganic Chemistry* 53: 8902-8912.
- Kim, K.S., Kwon, T.S., Yang, J.S. & Yang, J.W. 2007. Simultaneous removal of chlorinated contaminants by pervaporation for the reuse of a surfactant. *Desalination* 205: 87-96.
- Kumar, S.G. & Rao, K.S.R.K. 2015. Zinc oxide based photocatalysis: Tailoring surface-bulk structure and related interfacial charge carrier dynamics for better environmental applications. *RSC Advances* 5: 3306-3342.
- Laudadio, G. & Noël, T. 2021. *1 Photochemical Transformations in Continuous-Flow Reactors*. Walter de Gruyter GmbH.
- Liang, Q., Qiao, F., Cui, X. & Hou, X. 2019. Controlling the morphology of ZnO structures via low temperature hydrothermal method and their optoelectronic application. *Material Science and Semiconductor Processing* 89: 154-160.
- Liu, H., Hu, Y., Zhang, Z., Liu, X., Jia, H. & Xu, B. 2015. Synthesis of spherical Ag/ZnO heterostructural composites with excellent photocatalytic activity under visible light and UV irradiation. *Applied Surface Science* 355: 644-652.
- Maldonado, C., Fierro, J.L.G., Coronado, J., Sánchez, B. & Reyes, P. 2010. Title of Paper. *Journal of the Chilean Chemical Society* 55(3): 404-407.
- Martínez Vargas, D.X., De la Rosa, J.R., Lucio-Ortiz, C.J., Hernández-Ramírez, A., Flores-Escamilla, G.A. & García, C.D. 2015. Photocatalytic degradation of trichloroethylene in a continuous annular reactor using Cu-doped TiO₂ catalysts by sol-gel synthesis. *Applied Catalysis B: Environmental* 179: 249-261.
- Miao, J., Jia, Z., Lu, H.B., Habibi, D. & Zhang, L.C. 2014. Heterogeneous photocatalytic degradation of mordant black 11 with ZnO nanoparticles under UV-Vis light. *Journal of the Taiwan Institute of Chemical Engineers* 45: 1636-1641.
- Mittal, M., Sharma, M. & Pandey, O.P. 2016. Fast and quick degradation properties of doped and capped ZnO nanoparticles under UV-visible light radiations. *Solar Energy* 125: 51-64.
- Pavithra, M. & Jessie Raj, M.B. 2022. Synthesis of ultrasonic assisted co-precipitated Ag/ZnO nanorods and their profound anti-liver cancer and antibacterial properties. *Materials Science and Engineering: B* 278: 115653.

- Pongwan, P., Inceesungvorn, B., Wetchakun, K., Phanichphant, S. & Wetchakun, N. 2012. Highly Efficient visible-light-induced photocatalytic activity of Fe-doped TiO₂ nanoparticles. *Engineering Journal* 16(3): 13-16.
- Pudukudy, M. & Yaakob, Z. 2015. Facile synthesis of quasi spherical ZnO nanoparticles with excellent photocatalytic activity. *Journal of Cluster Science* 26: 1187-1201.
- Shenoy, S., Tarafder, K. & Sridharan, K. 2021. Bimetallic nanoparticles grafted ZnO hierarchical structures as efficient visible light driven photocatalyst: An experimental and theoretical study. *Journal of Molecular Structure* 1236: 130355.
- Su, Y., Straathof, N.J.W., Hessel, V. & Noël, T. 2014. Photochemical transformations accelerated in continuous-flow reactors: Basic concepts and applications. *Chemistry - A European Journal* 20(34): 10562-10589.
- Sukriti, Chand, P., Singh, V. & Kumar, D. 2020. Rapid visible light-driven photocatalytic degradation using Ce-doped ZnO nanocatalysts. *Vacuum* 178: 109364.
- Veerakumar, P., Sangili, A., Saranya, K., Pandikumar, A. & Lin, K.C. 2021. Palladium and silver nanoparticles embedded on zinc oxide nanostars for photocatalytic degradation of pesticides and herbicides. *Chemical Engineering Journal* 410: 128434.
- Wang, K.H., Jehng, J.M., Hsieh, Y.H. & Chang, C.Y. 2002. The reaction pathway for the heterogeneous photocatalysis of trichloroethylene in gas phase. *Journal of Hazardous Materials* 90(1): 63-75.
- Wang, J., Jiang, Z., Zhang, Z., Xie, Y., Lv, Y., Li, J., Deng, Y. & Zhang, X. 2009. Study on inorganic oxidants assisted sonocatalytic degradation of acid red B in presence of nano-sized ZnO powder. *Separation and Purification Technology* 67: 38-43.
- Wang, J., Jiang, Z., Zhang, Z., Xie, Y., Wang, X., Xing, Z., Xu, R. & Zhang, X. 2008. Sonocatalytic degradation of acid red B and rhodamine B catalyzed by nano-size ZnO powder under ultrasonic irradiation. *Ultrasonics Sonochemistry* 15: 768-774.
- Wu, B., Li, J. & Li, Q. 2019. Preparation and photoluminescence behavior of Mn-doped nano-ZnO. *Optik* 188: 205-211.

*Corresponding author; email: pummarin.k@chula.ac.th